Identifying reflected waves in passive microseismic data

C. Demerling*, S. Maxwell, and T. Urbancic
1 Hyperion Court, Kingston, ON, K7K 7G3
christina.demerling@esg.ca

ABSTRACT
Passive borehole microseismic activity emanates from a hydrocarbon reservoir due to changes in stress (either increase or decrease) and is monitored with a string of triaxial geophones in a monitoring well, installed either permanently (for reservoir monitoring) or on wireline (for hydraulic fracture mapping). Maxwell and Urbancic (2001) and Maxwell *et al* (2002) summarise the many applications of passive microseismic monitoring to petroleum production: mapping the extent of fracturing during hydraulic fracture treatments; fault mapping; tracking the gas or water front for assisted recovery production; monitoring casing deformation; and mapping the thermal front of heavy oil production.

Microseismic event origin locations are calculated from the moveout of and arrival time difference between P- and S-wave arrivals, and also from hodograms.

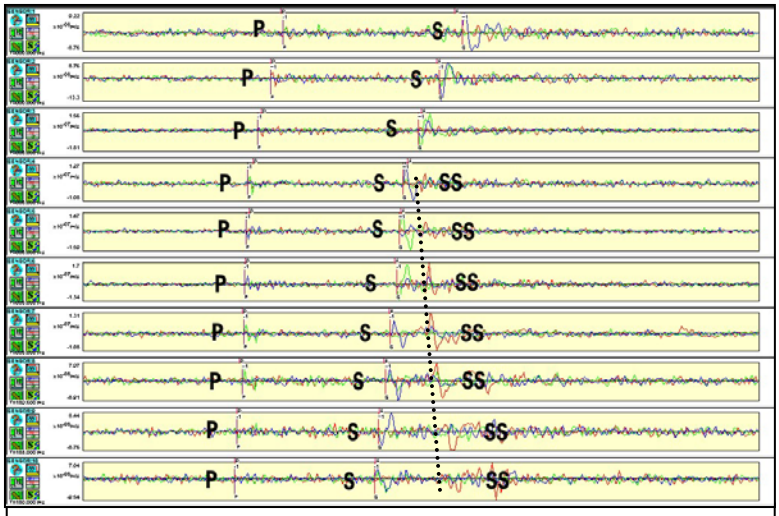

*Fig. 1: Seismic traces of a microseismic event, showing clear P- (**P**), S- (**S**) and reflected S- (**SS**) wave arrivals, traces are 262 ms long.*

In some cases of passive monitoring for hydraulic fracture treatments, P-wave arrivals have very low energy or are obscured by ambient noise and calculating accurate event origins is not possible. In a few of these same cases, lithological characteristics are present that create reflected waves that may be used to constrain event hypocentres (see *Fig. 1*). The focus of this research is to determine whether and how reflected energy can be used to add value to datasets with poor P-wave energy. The reflected wave also shows great promise in permanent reservoir monitoring for analysis of anisotropy related to production (Caley *et al*, 2001), monitoring reservoir drainage, and improving the earth model.

This research involved the following phases: data selection (with good quality arrivals for all three phases of interest that have reliable origin locations); verification of the reflecting interface depth and velocity model; identification of

the direct and reflected wave; and development of a new processing algorithm that uses both direct and mode-converted waves to locate hypocentres of microseismic events.

Fig. 1 shows seismic traces of a microseismic event, recorded by a vertical string of triaxial geophones, with clear arrivals from direct P- and S-waves and reflected S-waves. For illustration purposes, *Fig. 2* shows the raypaths of S-waves reflecting off of an interface and also the direct wave raypaths from the source to each of the triaxial geophones. Because the reflected wave first appears on the fourth geophone, the reflecting interface must lie between the 3rd and 4th geophones. A probable candidate for this reflecting interface is shown in *Fig. 3*, indicated by a velocity change at 7014'.

Fig. 3 shows the original velocity model used to locate the events, which was derived from a dipole sonic log and inversion of arrival times of microseismic data. For this study, a simplified two-layer, horizontal interface model was used to model the reflections. The revised velocities were calculated from weighted-averages of the original velocity model. It is important to note that the upper section of the original velocity model, from 6815' to 7275' (2077-2217 m), is faster on average by approximately 2000 ft/s (610 m/s) than the lower section (7275'-7500'). The weighted average velocities were verified by matching the P-S wave arrival time difference in the observed and calculated data, using the existing hypocentre to calculate raypath

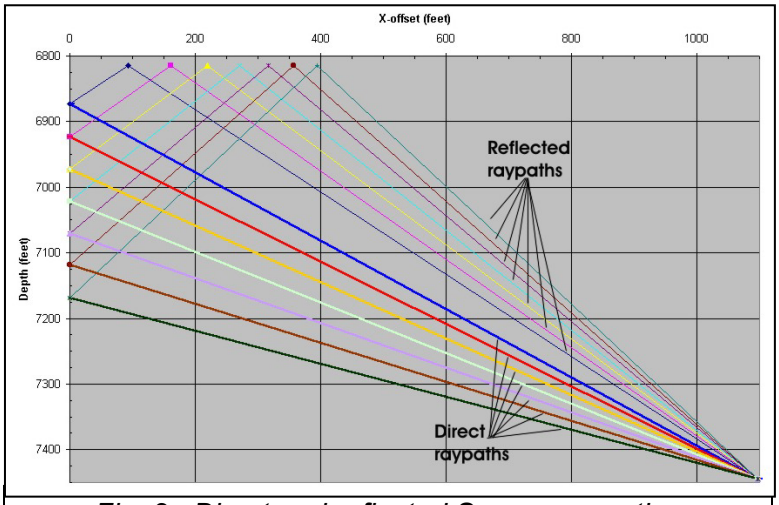

Fig. 2: Direct and reflected S-wave raypaths.

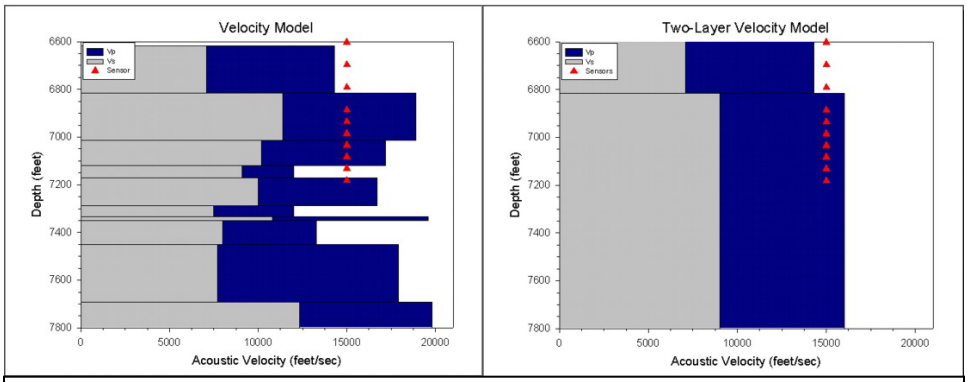

Fig. 3: Original layered velocity model and the simplified 2-layer velocity model used for reflection data processing.

lengths (as illustrated in *Fig. 2*). Depth of the reflecting interface was verified by matching the direct and reflected S-wave arrival time differences.

Initially, the same S-wave velocity (Vs=9000 ft/s (2743 m/s)) was used for direct wave and the upgoing and downgoing waves of the reflected wave; however, there was a poor match in the arrival time difference between the direct and reflected S-waves. To reflect the faster average velocities in the upper section of the lithology, the downgoing wave velocity was increased iteratively and produced arrival time differences in good agreement with observed ones when the downgoing wave velocity was 11500 ft/s (3505 m/s). In future applications, a detailed layered velocity model may be used for better location accuracy.

The arrival time differences for one event using the finalized parameters are shown in *Fig. 4*, and results from other events of the dataset had the same level of agreement. In summary, the reflecting interface depth was 6815' (2077 m), P-wave velocity was 16000 ft/s (4877 m/s), direct and upgoing S-wave velocity was 9000 ft/s (2743 m/s), and the reflected (downgoing) S-wave velocity was 11500 ft/s (3505 m/s).

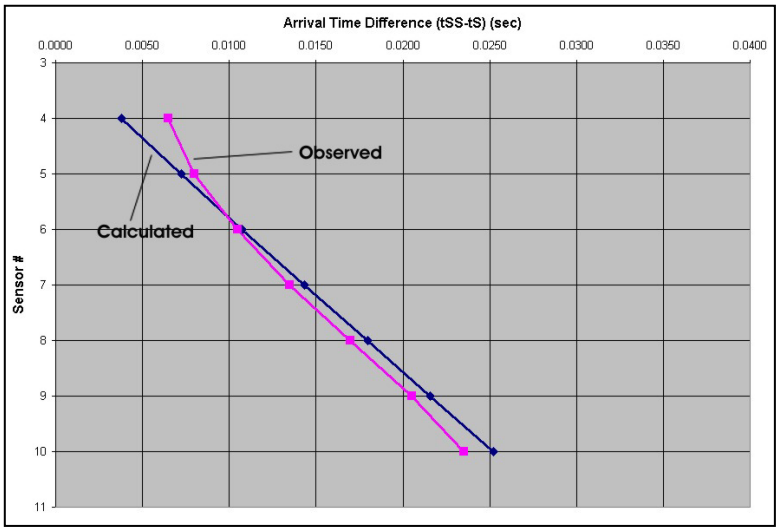

Fig. 4: Final observed and calculated arrival time difference between direct and reflected S-waves.

To determine whether the reflected S-wave may be used effectively to constrain hypocentres of microseismic events, the assumed event origin was perturbed +/- 40' (30.5 m) in offset and depth. The resulting calculated arrival time differences (shown in *Fig. 5*) indicate that they are sensitive enough to depth and offset errors that they can be used to constrain the correct location and lead to a reliable hypocentre location. A data processor is currently in development to exploit this sensitivity.

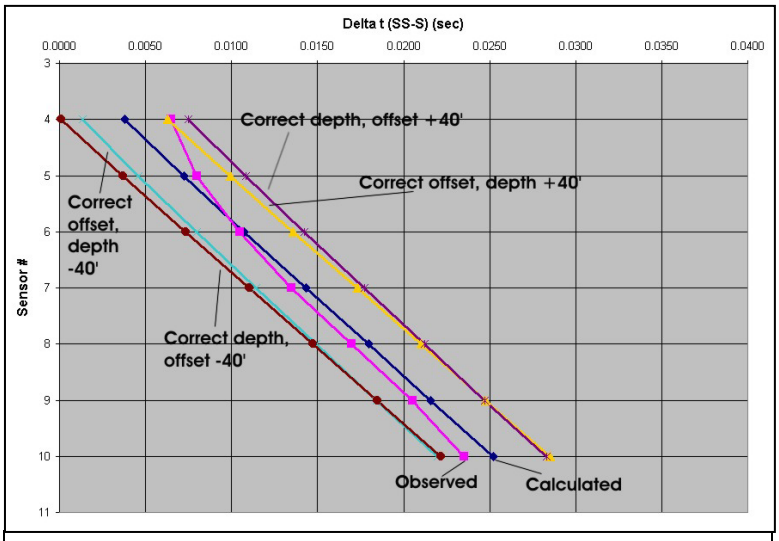

Fig. 5: Observed and calculated arrival time differences between direct and reflected S-waves affected by perturbations in assumed source location (depth and offset). The arrival time differences from incorrect source location assumptions envelope the correct solution.

In the future, this added value from passive microseismic monitoring could augment lithology and velocity models and help tie-in ongoing reservoir monitoring with discrete reflection seismic datasets. These reflected waves can be used to refine the earth model, which may impact reservoir volume estimates. Over time, the reflected waves can be used to map impedance changes both below and above the monitoring array, helping determine reservoir depletion and/or extent of gas/water flooding. These waves may also be used as a passive VSP survey with a shear wave source, possibly to be used in AVO analysis. The S-waves may also be used to determine fracture density and orientation through anisotropy analysis (Caley *et al*, 2001).

References

Caley, A.J., Kendall, J.-M., Jones, R.H., Barkved, O.I., Folstad, P.G. 2001. Monitoring Fractures in 4D Using Microseismic Data. EAGE 63rd Conference and Technical Exhibition. Amsterdam, The Netherlands.

Maxwell, S.C. and Urbancic, T.I. 2001. The role of passive microseismic monitoring in the instrumented oil field. The Leading Edge. Vol. 20. pp. 636-639. Society of Exploration Geophysicists. Tulsa, OK, U.S.A.

Maxwell, S.C., Urbancic, T.I., Prince, M. 2002. Passive Seismic Imaging of Hydraulic Fractures. CSEG National Convention. Calgary, Canada.

Sheriff, R.E. and Geldart, L.P. 1995. Exploration Seismology. 2nd ed. Cambridge University Press, U.S.A. pp. 33-99, 471-476.